COBEM 99
XV Congresso Brasileiro de Engenharia Mecânica
15th Brazilian Congress of Mechanical Engineering
22 - 26 de Novembro de 1999 / November 22 - 26, 1999 Águas de Lindóia, São Paulo,

THE INFLUENCE OF NUMERICAL PARAMETERS ON UNSTEADY AIRFOIL INVISCID FLOW SIMULATIONS USING UNSTRUCTURED DYNAMIC MESHES

Carlos Frederico Castro Simões
EMBRAER - Empresa Brasileira de Aeronáutica, Av. Brigadeiro Faria Lima, 2170
12227-901 - São José dos Campos - SP - BRAZIL
João Luiz Filgueiras Azevedo
Instituto de Aeronáutica e Espaço, CTA/IAE/ASE-N
12228-904 - São José dos Campos - SP - BRAZIL

Abstract*. The efforts for the simulation of unsteady airfoil flows using an unstructured finite volume algorithm are described. The flowfield is modeled using the inviscid equations of gasdynamics, i.e., the Euler equations, which are discretized in a cell centered unstructured grid made up of triangles. The work is focused on unsteady calculations for NACA 0012 airfoil at transonic flow conditions, by means of comparisons of results obtained with different time-stepping schemes and mesh refinement levels. All results are compared to experimental and numerical data found on the literature.*

Keywords:*Unsteady flow, Unstructured mesh, Finite volume method, Aerodynamic hysteresis.*

1. INTRODUCTION

Computational methods for the treatment of aerodynamic problems have evolved to a point in which the simulation of rather realistic flow situations is attainable with acceptable accuracy and computational costs.

The treatment of a truly complex configuration would usually require the use of one of two approaches. The first option would be the use of multiple block grid strategies, if one would insist on working with structured meshes. But even with such an approach, it could be difficult to avoid the waste of many grid points in regions of negligible spatial gradients. A much more general approach for the treatment of complex geometries would be the use of unstructured grids composed, for instance, of triangles in two-dimensions or tetrahedra in 3-D.

The present work is concerned with the development of a two-dimensional, unstructured, finite volume Euler solver with the capability of treating unsteady aerodynamic flows. The emphasis of the work is on pitching airfoil flow simulations but as it is usually the case with unsteady calculations, an initial steady state solution for the mean flight condition of interest has to be obtained.

Some parameters related to mesh refinement, artificial dissipation and time-stepping scheme have fundamental influence on the solutions. The aim of this work is to analyze this influence by means of comparisons between the results and experimental data. Finally, concluding remarks will be drawn indicating the current status of the work and the proposed lines for extension of the present effort.

2. THEORETICAL FORMULATION AND SPACE DISCRETIZATION

The two-dimensional, time-dependent Euler equations can be written in integral form for 2-D Cartesian coordinates as

$$\frac{\partial}{\partial t}\iint_V Q\ dxdy + \int_S (Edy - Fdx) = 0\,. \tag{1}$$

Here, V represents the area of the control volume and S is its boundary. The vector of conserved quantities, Q, is written as

$$Q = \begin{Bmatrix} \rho \\ \rho u \\ \rho v \\ e \end{Bmatrix}. \tag{2}$$

For a non-stationary mesh the inviscid flux vectors, E and F, are given by

$$E = \begin{Bmatrix} \rho U \\ \rho u U + p \\ \rho v U \\ (e+p)U + x_t p \end{Bmatrix} \qquad F = \begin{Bmatrix} \rho V \\ \rho u V \\ \rho v V + p \\ (e+p)V + y_t p \end{Bmatrix}. \tag{3}$$

The contravariant velocity components are defined as

$$U = u - x_t\,, \qquad V = v - y_t\,, \tag{4}$$

where x_t and y_t represents the Cartesian velocity components of the mesh.

The 2-D Euler equations in integral form are discretized by a finite volume procedure in an unstructured grid made up of triangles. The present algorithm is a cell centered scheme in which the variables actually stored represent an average over the control volume of the conserved quantities. The Euler equations can, then, be rewritten for each i-th control volume as

$$\frac{\partial}{\partial t}(V_i Q_i) + \int_{S_i} (Edy - Fdx) = 0\,. \tag{5}$$

We must point out that the interface flux computation used in the present work is somewhat different from that used by the authors in a previous work (Simões & Azevedo, 1997). The approach here is the same used by Jameson *et al.* (1981), i.e., for a cell centered scheme, these authors compute the average of the conserved variables at the interface and, then, form the interface flux using these averaged quantities.

The Euler equations are a set of nondissipative hyperbolic conservation laws. Hence, their numerical solution requires the introduction of artificial dissipation terms in order to avoid oscillations near shock waves and to damp high frequency uncoupled error modes. In the present work, the numerical dissipation terms are formed as a careful blend of undivided Laplacian and biharmonic operators (Batina, 1989). Hence, the artificial dissipation operator, $D(Q_i)$, can be written as

$$D(Q_i) = d^{(2)}(Q_i) - d^{(4)}(Q_i), \tag{6}$$

where $d^{(2)}(Q_i)$ represents the contribution of the undivided Laplacian operator, and $d^{(4)}(Q_i)$ the contribution of the biharmonic operator. The biharmonic operator is responsible for providing the background dissipation to damp high frequency uncoupled error modes and the undivided Laplacian artificial dissipation operator prevents oscillations near shock waves.

Therefore, the Euler equations, fully discretized in space and after the explicit addition of artificial dissipation terms, can be written as

$$\frac{d}{dt}(V_i Q_i) + C(Q_i) - D(Q_i) = 0. \tag{7}$$

3. TIME DISCRETIZATION

The semi-discrete equations are advanced in time using a second-order accurate, 5-stage, explicit, hybrid scheme which evolved from the considerations of Runge-Kutta time stepping schemes. This scheme, already including the necessary terms to account for changes in cell area due to mesh motion or deformation, can be written as

$$\begin{aligned} Q_i^{(0)} &= Q_i^{(n)} \\ Q_i^{(l)} &= \frac{V_i^n}{V_i^{n+1}} Q_i^{(0)} - \alpha_l \frac{\Delta t_i}{V_i^{n+1}} \left[C(Q_i^{(l-1)}) - D(Q_i^{(m)}) \right] \quad , \quad l = 1,\ldots,5 \rightarrow \begin{bmatrix} l = 1 \rightarrow m = 0 \\ l > 1 \rightarrow m = 1 \end{bmatrix} . \\ Q_i^{(n+1)} &= Q_i^{(5)} \end{aligned} \tag{8}$$

The values used for the α coefficients, as suggested by Mavriplis (1990), are

$$\alpha_1 = \frac{1}{4}, \quad \alpha_2 = \frac{1}{6}, \quad \alpha_3 = \frac{3}{8}, \quad \alpha_4 = \frac{1}{2}, \quad \alpha_5 = 1. \tag{9}$$

We observe that the convective operator, $C(Q)$, is evaluated at every stage of the integration process, but that the artificial dissipation operator, $D(Q)$, is only evaluated at the two initial stages. As discussed by Jameson *et al.* (1981), this type of procedure is known to provide adequate numerical damping characteristics while achieving the desired reduction in computational cost.

In order to verify the influence of the method used in time discretization procedure, another two time-stepping schemes were tested. The first one is a second-order accurate, 4-stage, explicit, hybrid scheme (Batina, 1989) which can be written as

$$
\begin{aligned}
& Q_i^{(0)} = Q_i^{(n)} \\
& Q_i^{(l)} = \frac{V_i^n}{V_i^{n+1}} Q_i^{(0)} - \alpha_l \frac{\Delta t_i}{V_i^{n+1}} \left[C(Q_i^{(l-1)}) - D(Q_i^{(0)}) \right] \quad , \quad l = 1, \ldots, 4 \rightarrow \begin{bmatrix} l = 1 \rightarrow m = 0 \\ l > 1 \rightarrow m = 1 \end{bmatrix} . \\
& Q_i^{(n+1)} = Q_i^{(4)}
\end{aligned}
\tag{10}
$$

The values used for the α coefficients are

$$
\alpha_1 = \frac{1}{4} , \quad \alpha_2 = \frac{1}{3} , \quad \alpha_3 = \frac{1}{2} , \quad \alpha_4 = 1 .
\tag{11}
$$

For this method, the convective operator, *C(Q)*, is evaluated at every stage of the integration process, but the artificial dissipation operator, *D(Q)*, is only evaluated at the first stage.

Finally, the authors tested the second-order accurate, explicit, Runge-Kutta time stepping scheme, in its simplest form, which can be written as

$$
\begin{aligned}
& Q_i^{(n+\frac{1}{2})} = \frac{V_i^n}{V_i^{n+1}} Q_i^{(n)} - \alpha_1 \frac{\Delta t_i}{V_i^{n+1}} \left[C(Q_i^{(n)}) - D(Q_i^{(n)}) \right] \\
& Q_i^{(n+1)} = \frac{V_i^n}{V_i^{n+1}} Q_i^{(n)} - \alpha_2 \frac{\Delta t_i}{V_i^{n+1}} \left[C(Q_i^{(n)}) - D(Q_i^{(n)}) + C(Q_i^{(n+\frac{1}{2})}) - D(Q_i^{(n+\frac{1}{2})}) \right]
\end{aligned} .
\tag{12}
$$

The values used for the α coefficients are

$$
\alpha_1 = 1 , \quad \alpha_2 = \frac{1}{2} .
\tag{13}
$$

As previously mentioned, steady state solutions for the mean flight condition of interest must be obtained before the unsteady calculation can be started. Therefore, it is also important to guarantee an acceptable efficiency for the code in steady state mode. This efficiency was achieved here by using a local time stepping option. The objective in implementing this option is to keep an approximately constant CFL number throughout the whole field. The implementation here is the same used by the authors in previous work (Simões & Azevedo, 1997).

4. BOUNDARY CONDITIONS

All boundary conditions were implemented with the use of "ghost", or "slave", cells. These are fictitious control volumes which are defined outside the computational domain of interest and which serve the solely purpose of implementing boundary conditions. Two types of boundary conditions must be considered for the airfoil applications emphasized in the present work. These are solid wall and far field boundary conditions.

At a solid wall boundary, the flow must be tangent to the wall in the inviscid case. This is enforced here by imposing that the velocity component normal to the wall in the ghost volume has the same magnitude and opposite sign of the normal velocity component in its adjacent interior volume, whereas the ghost volume velocity component tangent to the wall is exactly equal to its internal cell counterpart. The other two conditions are obtained by assuming a zero normal pressure gradient and a zero normal temperature gradient at the wall.

The correct treatment of far-field boundaries should implement non-reflective boundary conditions that should allow for the undisturbed propagation of outward going waves. This was accomplished in the present work with the use of one-dimensional Riemann invariants (Jameson & Baker, 1983).

5. GRID GENERATION AND DYNAMIC MESH ALGORITHM

An advancing front type grid generation scheme was implemented which is capable of automatic generation of 2-D unstructured meshes composed of triangles. The procedure can be divided in four separated phases, which are the generation of nodes, triangulation, grid smoothing and adaptative refinement.

The first step of the procedure described above is accomplished by generating a structured parabolic mesh around the airfoil. The obtained nodes are then used on the subsequent generation phases. Being so, the final unstructured mesh carries some structured grid inconveniences, as high cell skewness values and excessive number of nodes near the far field boundary. Fig. 1 shows a mesh around NACA0012 airfoil generated using the advancing front type generation scheme.

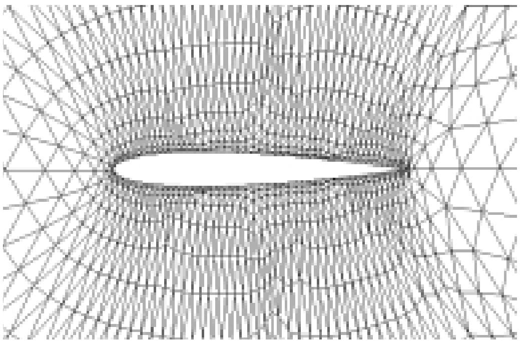

Fig. 1: Mesh #1 - 3468 nodes, 6732 cells, 102 farfield nodes, 102 profile nodes - Advancing front method

In order to verify the grid quality influence on the results, another two unstructured meshes were generated using the commercial package Geomesh (Fluent, 1997). The grid quality of those meshes are much better in terms of cell skewness, area variation and selective refinement. Figs. 2 to 3 show two meshes around NACA0012 airfoil generated using Geomesh.

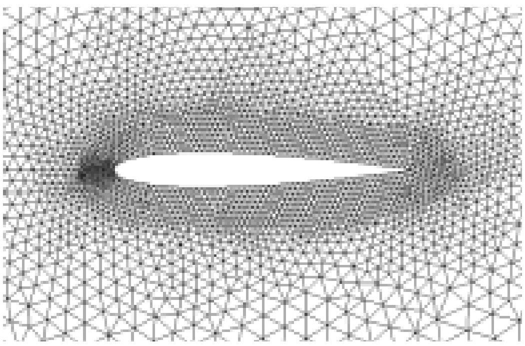

Fig. 2: Mesh #2 - 5024 nodes, 9920 cells, 22 farfield nodes, 106 profile nodes - Geomesh

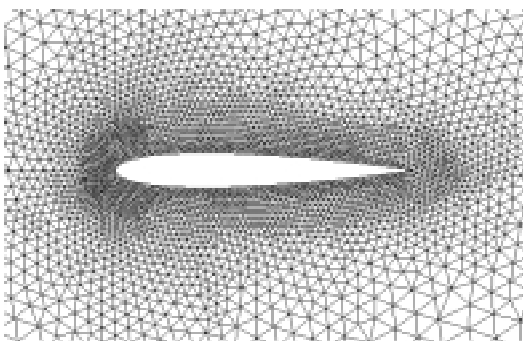

Fig. 3: Mesh #3 - 5908 nodes, 11634 cells, 22 farfield nodes, 160 profile nodes - Geomesh

Unsteady calculations involve airfoil motion and, therefore, the computational grid should be somehow adjusted to take this motion into account. The approach adopted here is to keep the far field boundary fixed and to move the interior points in order to accommodate the prescribed motion of the airfoil points. This was done following the ideas presented by Batina (1989), in which each side of the triangle is modeled as a spring with stiffness constant proportional to the length of the side. Hence, once points on the airfoil surface have been moved, and if we assume that far field points are held fixed, a set of static equilibrium equations can be solved for the position of the interior grid points. This technique was the same used by Oliveira (1993) and it is important to emphasize that the grid quality of the resulting mesh is maintained by this approach.

6. CALCULATION OF STEADY AIRFOIL FLOWS

The steady flow cases treated by the authors considered both fully subsonic and transonic airfoil flows. Steady state pressure coefficient distributions for subcritical and transonic flow cases over a NACA 0012 airfoil were compared by the authors in previous work to some results found on literature. The comparisons show very good agreement between the results and the literature (Simões & Azevedo, 1997).

7. SIMULATIONS OF UNSTEADY FLOWS

Unsteady calculations were performed for NACA 0012 airfoils at various transonic flow conditions. The simulations have considered harmonic oscillations about the airfoil quarter-chord. In all cases, the airfoil motion was prescribed and the interest was in calculating the aerodynamic response in terms of unsteady pressure distributions and aerodynamic coefficients. The usual procedure followed in the present work was to obtain a steady state solution for a certain flight condition of interest and, then, to start the unsteady motion from this converged solution.

In the case of harmonic motion, it is clear that this procedure will cause some initial numerical transients since the initial conditions for the unsteady motion are not exactly equal to those of the converged steady state solution. These initial transients were evaluated for the case of a sinusoidal pitch motion about the quarter-chord of a NACA 0012 airfoil (freestream Mach number M_∞=0.755, mean angle of attack α_0=0.016°, oscillation amplitude $\Delta\alpha$=2.51°, reduced frequency k=0.0814) and they are shown at Figs. 4 and 5. The results were obtained using mesh #3 previously presented.

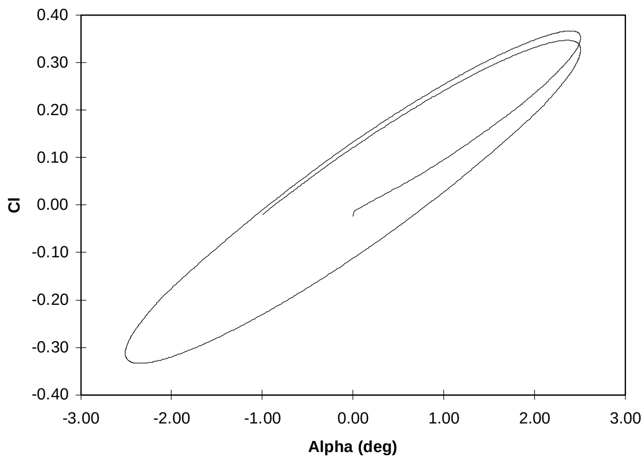

Fig. 4: Effect of initial transients on lift coefficient loops for a sinusoidal pitch motion

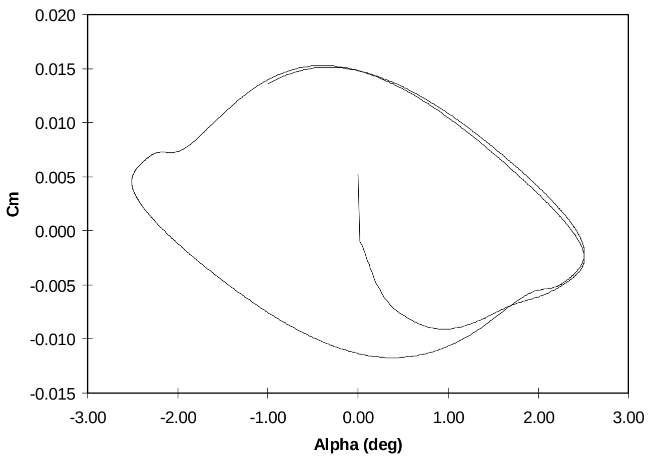

Fig. 5: Effect of initial transients on moment coefficient loops for a sinusoidal pitch motion

The important conclusion from these results is that the data on the first cycle of oscillation are contaminated by the initial transients and they should not be used to provide harmonic airfoil response. It is clear that, if one is only interested in harmonic responses, the effect of this numerical transient would die out together with the effects previously discussed. However, there are applications in which one may be interested in having a converged time-accurate unsteady response from the beginning of the motion. In these cases, this type of numerical transient must be eliminated.

As previously mentioned, three time stepping schemes were used to study the unsteady cases. As presented in previous work (Simões & Azevedo, 1997), the idea here is to verify possible different phase errors in the Runge-Kutta schemes. However the results obtained for all schemes were virtually the same and correspond to the hysteresis curves already shown at Figs. 4 and 5, for mesh #3.

Another numerical parameter verified was the grid quality. All previously presented meshes were used on the unsteady calculations and the results were compared, as shown at Figs. 6 and 7. The hysteresis curves are compared to experimental data (Landon, 1982) and numerical results found in the literature (Batina, 1989).

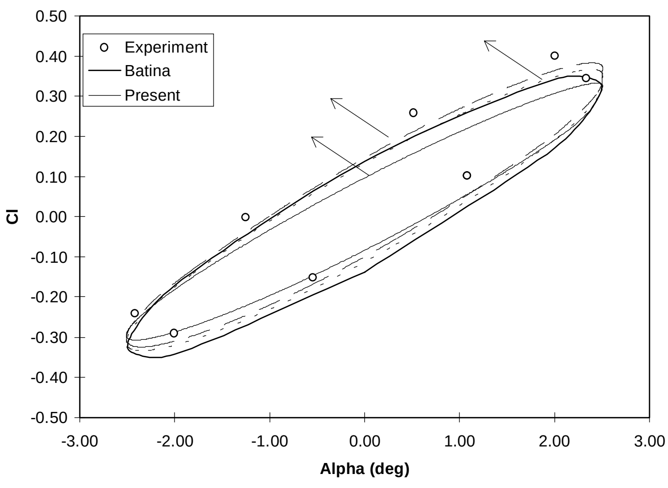

Fig. 6: Comparison of lift coefficient hysteresis loops with results from the literature

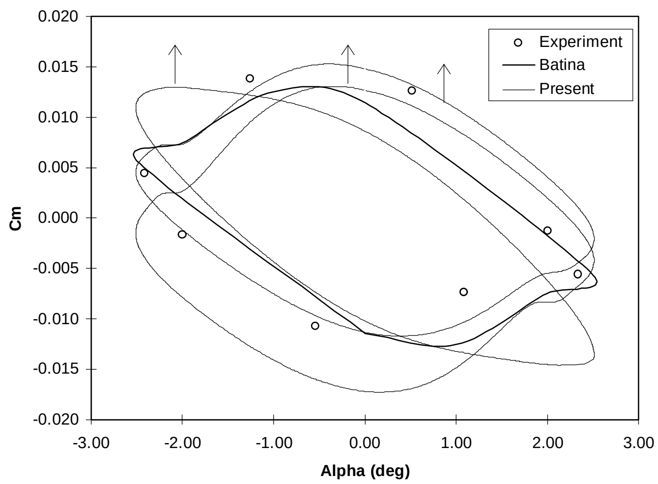

Fig. 7: Comparison of moment coefficient hysteresis loops with results from the literature

It is clear from the figures that the agreement of the mesh #1 results with the experimental data is not as good as one would like to have, but for mesh #2 and mesh #3, the agreement is much better. The main reason of these strong differences noted for mesh #1, from the authors standpoint, is its poor quality in terms of cell skewness and volume variation. Mesh #2 and mesh #3, though, have better grid quality and the nodes are more concentrated near the airfoil surface, avoiding excessive and useless node concentration near the far field boundary.

The fundamental difference between mesh #2 and mesh #3 is the number of nodes lying on the profile surface, which is greater for the last mesh. This is reflected on better agreement between its results and the experimental data, as a better shock definition is provided by mesh #3 which, in turn, leads to a more exact aerodynamic coefficient calculation.

A close look at the hysteresis loops reveals that some curves are not totally symmetrical. Though there is a slight asymmetry on the generated unstructured meshes, this could not generate so much aerodynamic coefficient asymmetry. The exact implications of this fact have not yet been fully explored at this point and it is the next investigation to be performed by the authors. Finally, it must be pointed out that the aerodynamic coefficients are very sensitive to shock location and the details of shock/boundary layer interaction may affect them significantly, causing the discrepancies between the present results and the experimental ones. It is important to emphasize that the present results correspond to simulations of the Euler equations and those shock/boundary layer interactions cannot be modeled.

8. CONCLUDING REMARKS

A finite volume procedure based on triangular unstructured grids was developed for the solution of the 2-D unsteady Euler equations in conservation form. Details of the spatial and temporal discretizations were presented, and aspects concerning artificial dissipation, convergence acceleration and implementation of boundary conditions were discussed. The grid generation and dynamic mesh motion algorithms were also briefly discussed. Unsteady transonic NACA 0012 airfoil flow results were also presented and discussed, with focus on time stepping scheme and grid quality influence on the results. In general, the results have shown good agreement with the available data. There was noted no influence of the used time stepping scheme, but a strong influence of the grid quality on the results. The application of the algorithm for more general airfoil motions is presently being considered. Its use to provide unsteady aerodynamic data for transonic aeroelastic analyses is the next logical step as an extension of the present effort.

Acknowledgments

The present work was partially supported by CNPq under the Integrated Project Research Grant No. 522413/96-0. Partial support has also been provided by EMBRAER - Empresa Brasileira de Aeronáutica S.A.

REFERENCES

Batina, J.T., 1989, Unsteady Euler Airfoil Solutions Using Unstructured Dynamic Meshes, AIAA Paper 89-0115, 27th Aerospace Sciences Meeting, Reno, NV.

Fluent, Inc., 1997, Geomesh User's Guide, Lebanon, NH.

Jameson, A. & Baker, T.J., 1983, Solution of the Euler Equations for Complex Configurations, AIAA Paper 83-1929.

Jameson, A. & Mavriplis, D. ,1986, Finite Volume Solutions of the Two-Dimensional Euler Equations on a Regular Triangular Mesh, AIAA Journal, Vol. 24, No. 4, pp. 611-618.

Jameson, A., Schmidt, W. & Turkel, E., 1981, Numerical Solution of the Euler Equations by Finite Volume Methods Using Runge-Kutta Time-Stepping Schemes, AIAA Paper 81-1259, AIAA 14th Fluid and Plasma Dynamics Conference, Palo Alto, CA.

Landon, R.H., 1982, NACA 0012, Oscillating and Transient Pitching, Data Set 3 in AGARD R-702, Compendium of Unsteady Aerodynamic Measurements.

Mavriplis, D.J., 1988, Multigrid Solution of the Two-Dimensional Euler Equations on Unstructured Triangular Meshes, AIAA Journal, Vol. 26, No. 7, pp.824-831.

Mavriplis, D.J., 1990, Accurate Multigrid Solution of the Euler Equations on Unstructured and Adaptative Meshes, AIAA Journal, Vol. 28, No. 2, pp. 213-221.

Oliveira, L.C., 1993, Uma Metodologia de Análise Aeroelástica com Variáveis de Estado Utilizando Técnicas de Aerodinâmica Computacional, Tese de Mestrado, ITA - Instituto Tecnológico de Aeronáutica, São José dos Campos, SP, Brazil.

Simões, C.F.C. & Azevedo, J.L.F, 1997, Unsteady Airfoil Inviscid Flow Simulations Using Unstructured Dynamic Meshes, XIV Congresso Brasileiro de Engenharia Mecânica, Bauru, SP, Brasil.